Unsteady Travel Behavior in Major and Minor Scale Disasters

Dharmarathna W.R.S.S.[1] and Eiji HATO[2]

[1] PhD candidate, Dept. of Civil Eng., The University of Tokyo
(7-3-1 Hongo, Bunkyo-ku, Tokyo 113-8656, Japan)
E-mail: samal@trip.t.u-tokyo.ac.jp
[2]Member of JSCE, Professor, Dept. of Civil Eng., The University of Tokyo
(7-3-1 Hongo, Bunkyo-ku, Tokyo 113-8656, Japan)
E-mail: hato@civil.t.u-tokyo.ac.jp

Route choice behavior under disastrous conditions become more complex than usual in densified networks. Therefore, a better understanding of the situation and investigating the travel behavior have become essential for smoothing the traffic flow and securing the road capacity for emergency and evacuation vehicles. Hence, this paper is focused on understanding the link characteristics and detecting the traveller's behaviours by using global positioning system trajectories of probe taxi data collected during the great east Japan earthquake occurred on 11th March 2011 and a torrential downpour occurred on 23rd July 2013 in Tokyo. Scrutinized time-space diagrams along with geographic information system based cross sectional analysis showed the deviation of link characteristics from the normal conditions. The estimated parameters, travel time, right turn dummy variable and sequential discount rate, through $\beta -$ scaled recursive logit model reflected the change of traveller's cognition and behaviour.

Key Words : *route choice, travellers' behavior, probe taxi data, parameter estimation, disaster situations*

1. INTRODUCTION

Traffic networks are subjected to significant delays due to the disturbances and operational irregularities caused by the earthquakes, extreme weather events, crashes, constructions and so forth. These delays could cost human lives in emergency situations, in addition to consume traveller's time, fuel and increase environmental pollution. Further, in such a context, traveller's decision making process oscillates between global decisions and myopic decisions, which would ultimately lead them to travel more distance than usual at a lower speed with many direction changes to reach the destination. Hence, very accurate data collected through high standard technologies, and well-developed route choice models are necessary to understand the mechanism and detect the abnormal travel behaviors in disaster situations. This study is aimed to fulfill that gap in the literature.

Even though it is not given the immediate priority[1)], collecting accurate real time data within the disaster period and consecutive few hours become crucial for comprehensive studies. The data collected through questionnaire surveys and travel surveys might have accuracy problems due to the memory decay and the emotional trauma. Therefore, it is very important to use advanced data collecting techniques such as probe technology, where it gives the global positioning system (GPS) trajectories of trips. This study used probe taxi data collected in Tokyo during two different scale disasters, the great east Japan earthquake and a torrential downpour.

The pacific coast of Tohoku, Japan was hit by a massive earthquake of magnitude 9.0 - 9.1 on the Richter scale at 14:46 Japanese standard time (JST) on Friday, 11 March 2011 and is known as the great east Japan earthquake. The trains and Tokyo metropolitan expressway were suspended for safety checks and more than 5 million people faced difficulties in returning home.

The torrential downpour was occurred at Shibuya, Minato, Shinagawa and Setagaya areas in Tokyo on 23rd July 2013. The rainfall was started around 15:15 and ended around 16:35 JST. The high intense rainfall (100 – 150 mm/h) caused a flash flood which inundated some of the underpasses and depressions within the area up to a maximum flood height of 0.5 m. This caused the difficulties for cars and taxis which cross over the inundated areas and such travelers had to choose alternative routes.

Traveller's decision making process under these scenarios vary between myopic and global decisions over the network, and hence it should be investigated through an unsteady model. Accordingly, the recently introduced β – scaled recursive logit model[2) was used for the analysis. The rest of the paper is organized as follows. Section 2 detailed a literature review. Section 3 presented the model formulation. In section 4, case studies are explained with cross sectional analysis and parameter estimation results. Finally, section 5 concludes the paper.

2. LITERATURE REVIEW

The increasing frequency and intensity of natural disasters over the past decades[3) and frequently experiencing earthquakes, highlighted the necessity of disaster preparedness in transport systems. Given the fact that future weather will become more extreme, it is vital for planners and policy-makers to understand how it influences on travel behaviour to achieve a sustainable transport system in more extreme future climate[4).

Travellers are naturally preferred to decide the route before starting the trip by assuming a continuous service system without any unexpected events. Accordingly, most of the available route choice models such as C-Logit[5), Path-Size Logit[6) addressed the path probabilities based on the pre-trip scenario. However, in the context of a disaster, travellers are forced to change their original travel plans based on the prevailing network conditions and it is necessary to understand how they modify their travel behavior in reaction to the incident[7). Hence it is essential to adopt a dynamic approach in the route choice context.

Accordingly, dynamic approaches are being discussed in the literature (e.g., [8), [9), [10), [11)) and captured traveller's route choice behavior in dynamic and stochastic networks. Moreover, the drivers forward-looking decision-making mechanism has incorporated in sequential route choice models[12), [13), [14) by assuming that drivers reach destinations through successive link choices.

The recursive logit (RL) model[14) was proposed by incorporating the aforementioned knowledge to the infinite multinomial logit model in the context of the route choice analysis with the use of dynamic discrete choice models[15). The RL model was generalized by incorporating the concept of sequential time discount rate (β) and referred as $\beta -$ scaled recursive logit (β – SRL) model[2). $\beta -$ SRL model was used in this study and its formulation is explained in detail in the next section.

3. MODEL FORMULATION

The formulation of RL model[14) and β – SRL model[2) are detailed below.

(1) Recursive logit model

Consider a directed connected graph $G = (A, N)$ where A and N denote the set of links and the set of nodes respectively. The assumption is made as, a driver chooses a link a_{j+1} from the set of outgoing links $A(a_j)$ which maximizes the sum of instantaneous utility $u(a_{j+1}|a_j)$ associated with each link pair and expected downstream utility to the destination link d; $V^d(a_{t+1})$ that is given as a value function which is formulated via Bellman equation[16) as follows.

$$V^d(a_j) = \mathrm{E}\left[\max_{a_{j+1}\in A(a_j)}\{v(a_{j+1}|a_j;\theta) + V^d(a_{j+1}) + \mu\varepsilon(a_{j+1})\}\right] \quad \forall a_j \epsilon A \tag{1}$$

where, $v(a_{j+1}|a_j;\theta) = v(x_{a_{t+1}|a_t};\theta)$ is the deterministic utility component, $x_{a_{t+1}|a_t}$ is a vector of observed characteristics of the link pair (a_j, a_{j+1}) and θ is an unknown parameter vector to be estimated. The random term ε is assumed to be an independent and identically distributed (i.i.d.) extreme value type I with scale parameter μ, the dummy link for the destination d has no successor, and the union of the link set and dummy link is denoted as $\tilde{A} = A \cup d$. The probability of choosing a link a_{j+1} given state a_j is given by the multinomial logit model.

$$p(a_{j+1}|a_j) = \frac{e^{\frac{1}{\mu}\{v(a_{j+1}|a_j)+V(a_{j+1})\}}}{\sum_{a'_{j+1}\in A(a_j)} e^{\frac{1}{\mu}\{v(a'_{j+1}|a_j)+V(a'_{j+1})\}}} \tag{2}$$

(2) $\boldsymbol{\beta} -$ scaled recursive logit model

RL model was modified by including the concept of sequential time discount rate β, as a generalization of drivers' decision-making dynamics and a representation of the degree of spatial cognition of networks. Accordingly, re-formulated the equation (1) as below;

$$V^d(a_j) = \mathrm{E}\left[\max_{a_{j+1}\in A(a_j)}\{v(a_{j+1}|a_j;\theta) + \beta V^d(a_{j+1}) + \mu\varepsilon(a_{j+1})\}\right] \quad \forall a_j \epsilon A \tag{3}$$

β is the sequential time discount rate of the value function and it is assumed to be vary between zero and one. The transition probability from link a_j to a_{j+1} is given by the multinomial logit model;

$$p(a_{j+1}|a_j) = \frac{e^{\frac{1}{\mu}\{v(a_{j+1}|a_j)+\beta V(a_{j+1})\}}}{\sum_{a'_{j+1}\in A(a_j)} e^{\frac{1}{\mu}\{v(a'_{j+1}|a_j)+\beta V(a'_{j+1})\}}} \tag{4}$$

The decision making dynamics with respect to the different sequential time discount rates can be illustrated as below.

a) $\beta = 1$

In this case, drivers are able to evaluate the expected utility of forward space V and the instantaneous utility of the next link v with equal weights. Hence, when β equal to one, route choice behavior depends on global decision over network. Figure 1(a) shows the graphical representation of the situation.

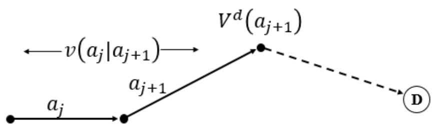

Fig.1(a) Graphical representation of $\beta = 1$ situation

b) $\beta = 0$

In this situation, drivers are supposed to myopically choose the next link based only on instantaneous utility v. Figure 1(b) indicates the graphical representation of the system.

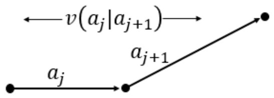

Fig.1(b) Graphical representation of $\beta = 0$ situation

c) $0 < \beta < 1$

This represents the intermediate situation between a) and b) where drivers could evaluate the expected utility of forward space V upto a certain extent. Figure 1(c) illustrates the situation.

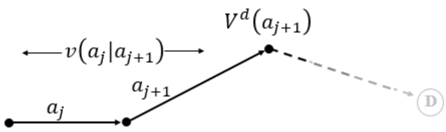

Fig.1(c) Graphical representation of $0 < \beta < 1$ situation

4. CASE STUDIES

In terms of traffic situation is concerned, two different scale disasters where travellers were forced to choose alternative routes, were considered as the case studies. The first case was the great east Japan earthquake occurred in 11th March 2011 and the other one was a torrential downpour occurred in 23rd July 2013.

A massive earthquake of magnitude 9.0 – 9.1 on the Richter scale was hit on the pacific coast of Tohoku area in Japan at 14:46 JST on Friday, 11 March 2011. The trains and Tokyo metropolitan expressway were suspended for safety checks and more than 5 million people faced difficulties in returning home. The site selected for this case study was the area belongs to the secondary mesh code 533946[17], which consisted 39,642 nodes and 54,211 links.

Shibuya, Minato, Shinagawa and Setagaya areas in Tokyo were affected by a torrential downpour on 23rd July 2013. The rainfall was started around 15:15 and ended around 16:35 JST. The high intense rainfall (100 – 150 mm/h) caused a flash flood which inundated some of the underpasses and depressions within the area up to a maximum flood height of 0.5 m. This caused the difficulties for cars and taxis which cross over the inundated areas and such travellers had to choose alternative routes. The site selected for this case study was the area belongs to the secondary mesh code 533935[17], which consisted 31,142 nodes and 38,180 links.

The behaviour characteristics under the aforementioned scenarios were investigated by using trajectory data of probe taxis collected during the disaster period and were compared with respective data correspond to exact one week period after the easch event. Accordingly, the probe taxi data corresponding to the dates 18th March 2011 and 30th July 2013 were used for the comparison purpose respectively for the earthquake and torrential downpour. Data were provided by the *vehicle information and communication system center*, which is an organization that collect and provide driver's road traffic information. The obtained probe GPS trajectories were map-matched based on the real road network data by using Dijkstra's algorithm[18] for the shortest path.

(1) Cross sectional analysis

The link characteristics were investigated through a cross sectional analysis, by scrutinizing the map-matched data. Since the both events were occurred in a much closer time in the afternoon session, the analysis being carried out from 14:00 to 18:00 hours on each day.

a) Time space diagram

Individual taxi movements during the disaster day and non-disaster day were compared by portraying sample trajectories on time-space diagrams. Figure 2(a) and 2(b) indicate example time-space diagrams under the torrential downpour and its normal condition while the figure 3(a) and 3(b) visualize the same under the great east Japan earthquake. Different colours illustrate the speed, which was averaged over the every two minutes of the trip. The trips were selected on the basis that they travelled similar directions from much closer origins to a closer destinations during the same time period on the respective days.

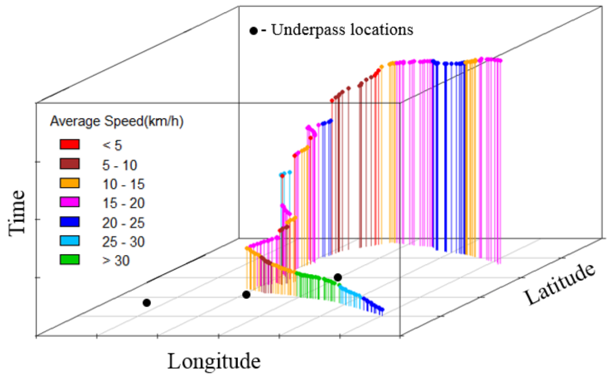

Fig.2(a) A sample taxi trajectory under torrential downpour

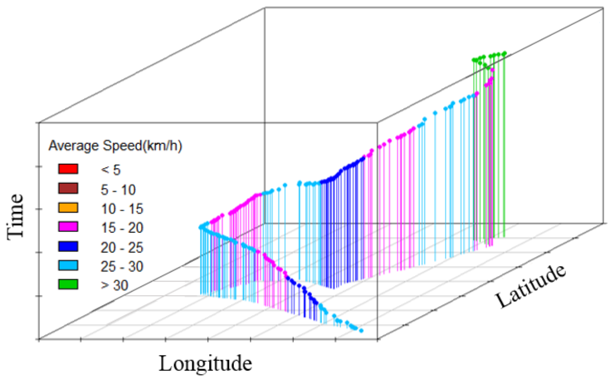

Fig.2(b) A sample taxi trajectory under normal condition

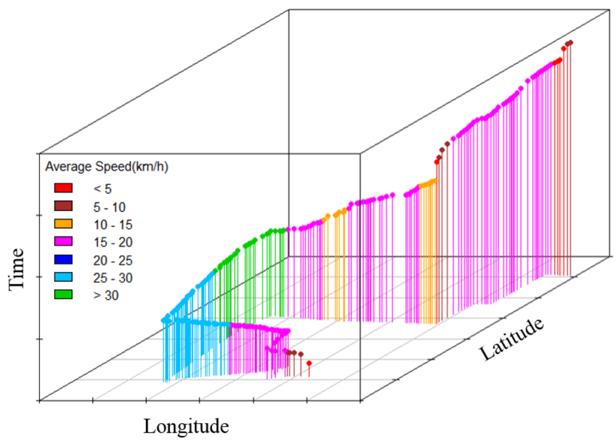

Fig.3(a) A sample taxi trajectory under earthquake condition

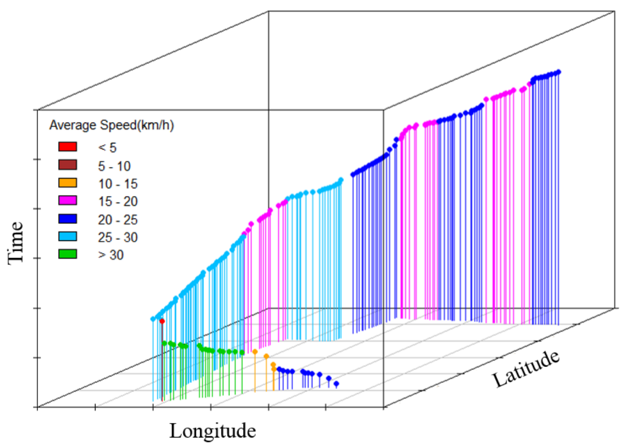

Fig.3(b) A sample taxi trajectory under normal condition

As per the figures 2(a) and 3(a), it can be visualized that travellers has reached the destinations through lengthier paths, with slower speeds and many direction changes, compared to the trips on figure 2(b) and 3(b) respectively.

b) Congestion index and speed

As far as the traffic behavior is concerned, the main difference between the two events is, torrential downpour only affected for the specific areas where the great east Japan earthquake influenced the entire network. Hence, in order to understand the congestion, average speed data under the torrential downpour was converted into congestion indexes (CI) by using the below relationship[19].

$$CI = \begin{cases} (V_{FF} - V)/V_{FF} & ;if\ V \leq V_{FF}\ and\ V_{FF} > 0 \\ 0 & ;if\ V > V_{FF} \end{cases} \tag{5}$$

where; $V -$ Average speed of the link, $V_{FF} -$ Free flow speed. The results indicated that the congestion indexes have increased forming the congestion around the underpasses and are summarised in table 1.

Table 1 Congestion indexes near the underpasses

Underpass No.	Congestion index	
	Disaster day	Normal day
3	0.4 – 0.8	0.2 – 0.6
4	0.6 – 1.0	0.0 – 0.4
8	0.6 – 1.0	0.2 - 0.6

The congestion occurred due to the great east Japan earthquake was visualized by using the averaged link speeds. Figure 4(a) and 4(b) show the comparison of average link speed between normal day and earthquake day from 14:00 to 18:00 hours.

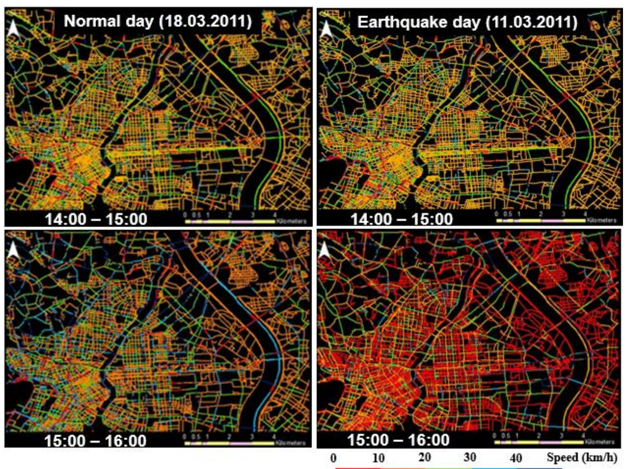

Fig.4(a) Speed variation from 14:00 to 16:00

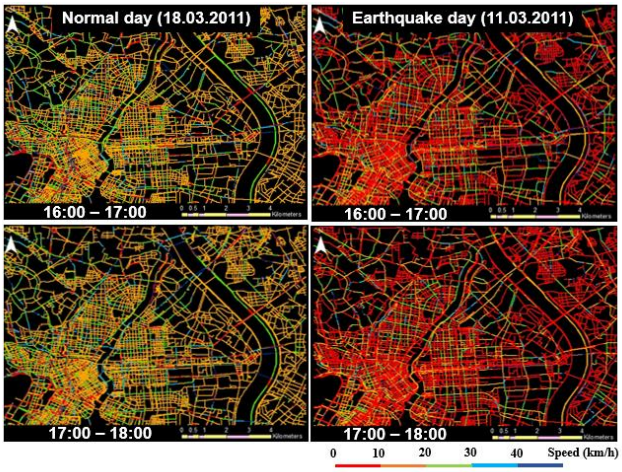

Fig.4(b) Speed variation from 16:00 to 18:00

Fig.4(a) and 4(b) clearly visualize the formation of congestion after the earthquake which was occurred by 14:46 hrs. It has congested heavily from the very next hour onwards, while the respective period looks quite normal in the other day.

c) Right-turn ratio

In the case of both events, travellers have to search for alternative routes and it cost more right turns as people drive on left in Japan. Accordingly, the speed tend to decrease and in order to investigate that, right turn ratios per node was plotted against the link speed. The comparison of downpour and earthquake are shown in the figure 5(a) and 5(b) respectively.

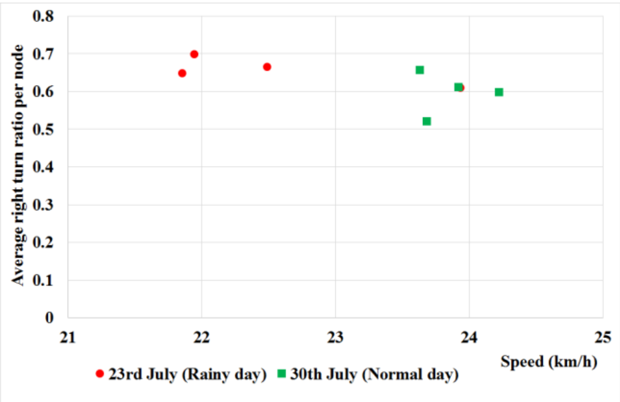

Fig.5(a) Variation of right turn ratio against speed under torrential downpour

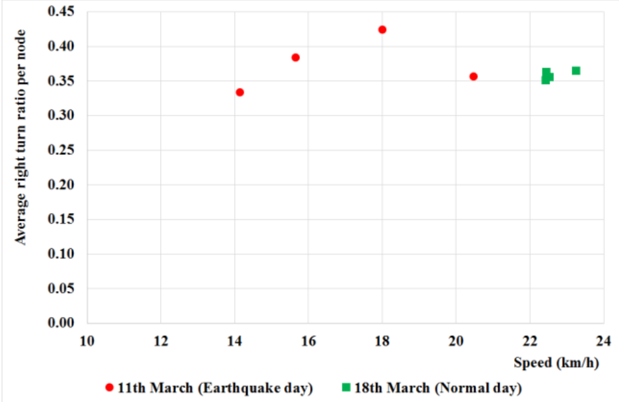

Fig.5(b) Variation of right turn ratio against speed under great east Japan earthquake

Fig.5(a) clearly indicates the difference between rainy condition and the normal condition. Under the rainy event, hourly right turn ratio per node lies between 0.65 to 0.70 while it is from 0.50 to 0.65 under the normal condition. The average speed was around 22 km/h on the rainy day while it was around 24 km/h on the normal day. In the fig.5(b) the time of the points that respect to the earthquake day are from 14:00 to 18:00 from the right to left. Hnece, it can be visualized the speed reduction as the time passes on after the earthquake and the right turn ratio per node also has reduced. This indicates the congestion during the time and difficulty of making right turns. On the other hand, the points respect to the normal day remains much close to each other during the considered period, which was from 14:00 to 18:00.

(2) Parameter estimation

The route choice behavior under the aforementioned disaster situations were investigated by estimating the parameters through $\beta-$SRL model. Three parameters were considered as travel time, right turn dummy variable and sequential time discount rate (β). Hourly simulations were carried out for four hours of period from 14:00 to 18:00 in all 4 days, torrential downpour day (23rd July 2013), respective normal day (30th July 2013), great east Japan earthquake day (11th March 2011) and respective normal day (18th March 2011). Two smaller areas were selected for the parameter estimation purpose and each consisted 3091 and 4608 links respectively under torrential downpour and the great east Japan earthquake. The estimation results under torrential downpour are shown in table 2 while the table 3 represented the same under the earthquake.

Table 2: Estimation results under the torrential downpour day and respective normal day

Date	**23rd July 2013**							
Time	14:00 – 15:00		15:00 – 16:00		16:00 – 17:00		17:00 – 18:00	
	Estimates	t-value	Estimates	t-value	Estimates	t-value	Estimates	t-value
Travel Time	-0.289	-4.65	-0.219	-4.81	-0.145	-4.87	-0.142	-4.70
Right turn	-0.598	-3.15	-0.345	-2.04	-0.529	-3.80	-0.844	-5.17
$\log(\beta/1-\beta)$	-0.251	-0.45	-0.870	-1.37	-1.446	-2.37	-0.727	-1.60
β	0.438	-	0.295	-	0.191	-	0.326	-
Sample		820		1085		1289		1347
Lc		-364.044		-372.180		-558.948		-546.656
LL		-258.284		-321.934		-514.953		-457.989
ρ^2		0.291		0.135		0.079		0.162
Date	**30th July 2013**							
Time	14:00 – 15:00		15:00 – 16:00		16:00 – 17:00		17:00 – 18:00	
	Estimates	t-value	Estimates	t-value	Estimates	t-value	Estimates	t-value
Travel Time	-0.481	-4.99	-0.279	-3.57	-0.303	-4.26	-0.451	-4.56
Right turn	-0.651	-2.52	-0.292	-1.25	-0.927	-3.80	-0.879	-3.56
$\log(\beta/1-\beta)$	-0.402	-0.65	-3.426	-0.88	-0.214	-0.39	0.779	1.23
β	0.401	-	0.031	-	0.447	-	0.685	-
Sample		577		568		666		519
Lc		-210.282		-189.425		-289.759		-887.100
LL		-152.222		-177.513		-199.160		-162.593
ρ^2		0.276		0.063		0.313		0.817

Table 3: Estimation results under the great east Japan earthquake day and respective normal day

Date	**11th March 2011**							
Time	14:00 – 15:00		15:00 – 16:00		16:00 – 17:00		17:00 – 18:00	
	Estimates	t-value	Estimates	t-value	Estimates	t-value	Estimates	t-value
Travel Time	-0.244	-4.45	-0.238	-3.41	-0.122	-5.39	-0.016	-1.30
Right turn	-1.296	-4.89	-1.164	-3.15	-1.561	-7.24	-1.710	-7.52
$\log(\beta/1-\beta)$	0.146	0.32	0.577	0.81	-1.274	-2.05	-0.889	-1.98
β	0.536	-	0.640	-	0.219	-	0.291	-
Sample		584		294		861		1016
Lc		-411.234		-312.245		-389.897		-515.599
LL		-201.315		-94.673		-331.011		-425.087
ρ^2		0.510		0.697		0.151		0.175
Date	**18th March 2011**							
Time	14:00 – 15:00		15:00 – 16:00		16:00 – 17:00		17:00 – 18:00	
	Estimates	t-value	Estimates	t-value	Estimates	t-value	Estimates	t-value
Travel Time	-0.384	-4.83	-0.314	-4.44	-0.216	-3.27	-0.173	-2.48
Right turn	-0.873	-3.50	-1.078	-3.73	-0.890	-3.44	-0.644	-2.32
$\log(\beta/1-\beta)$	0.193	0.38	-1.299	-1.56	0.219	0.362	0.465	0.66
β	0.548	-	0.214	-	0.555	-	0.614	-
Sample		406		347		350		305
Lc		-361.780		-182.014		-314.969		-379.916
LL		-157.813		-151.536		-154.906		-126.955
ρ^2		0.564		0.167		0.508		0.666

The estimated parameter values for travel time variable and right turn dummy variable consistently indicated minus sign for all periods from 14:00 to 18:00 in all four days and are significant except two cases. The respective estimation results are then compared between the two events for each variable.

a) Travel time parameter

The respective parameter values under each disaster are being plotted and shown in the figure 6.

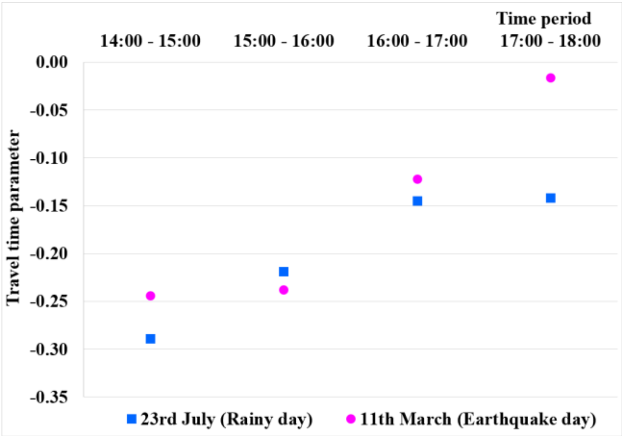

Fig.6 Variation of travel time parameter

The estimated values of the travel time parameter have increased under the both scenarios and it indicates the traveller's intention to assess the difference of travel time in links, under congestions. The rate of increasing is greater in the earthquake day, which reflect the vulnerability of situation and it has become extremely difficult to evaluate the link travel time during the period from 17:00 to 18:00.

b) Right turn dummy parameter

The estimated parameters are plotted in order to visualize the variation and shown in the figure 7.

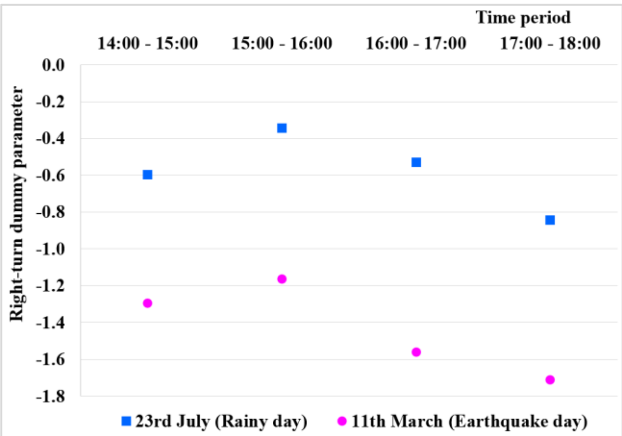

Fig.7 Variation of right turn dummy parameter

People drive on the left lane in Japan and obviously, reluctant to turn right. Hence, it becomes more significant under the congested scenarios. The fig.7 visualized that the estimated values of right turn dummy parameter has decreased after the occurrence of both events and it reflect the increasing difficulty in turning right. In addition, the magnitude of the values are high in the case of earthquake and it indicates the further difficulty in turning right under the circumstances.

c) Sequential time discount rate (β)

The sequential time discount rate indicates the oscillation of the traveler's decision making process between myopic and global. The respective estimations are plotted to observe this variation and showed in the figure 8.

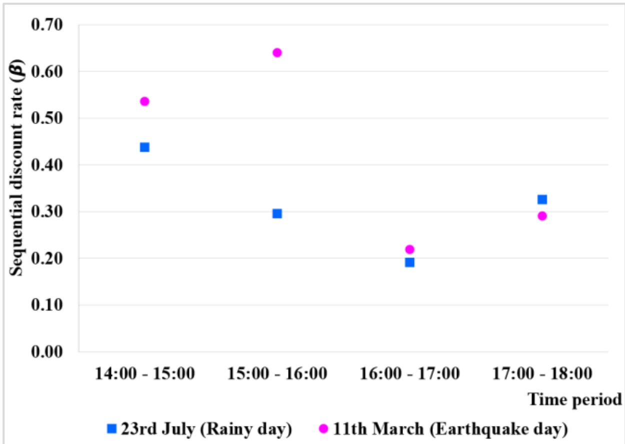

Fig.8 Variation of sequential time discount rate

After the unexpected massive earthquake and unpredicted suspension of trains and Tokyo metropolitan expressway, people were under panic situation and tried to maximize their global knowledge to choose the links. Hence, sequential time discount rate shows a higher value within the immediate hour after the earthquake. Even though, the enormous congestion forced them to turn on to the myopic decision process and accordingly, the sequential time discount rate become lower in the next hours. In the context of torrential downpour, as it was not heavily congested, the sequential time discount rate has gradually decreased.

Therefore, under the both scenarios, the sequential time discount rate has decreased and it reflects the changing tendency of human decision making behavior towards the myopic process. Figure 9 represents the graphical interpretation of aforementioned situation.

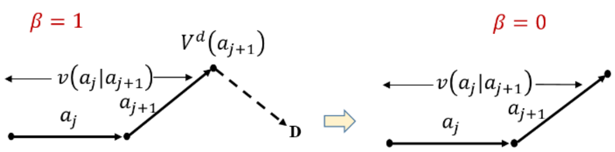

Fig.9 Graphical representation of the transition of sequential time discount rate

5. CONCUSIONS

The paper presents the traveller's abnormal travel behaviour under the influence of a major and a minor scale disasters in Tokyo, Japan. Probe taxi data, collected during the great east Japan earthquake occurred on 11th March 2011 and a torrential downpour occurred on 23rd July 2013, was used in the β −SRL, in order to understand the traveller's route choice behaviour. Scrutinized time-space diagrams showed that travelers reached their destinations through a lengthier paths, with slower speeds and many direction changes under the both disaster situations.

The congestion index analysis indicated that congestions have formed along the links which are connected to the inundated areas under the torrential downpour where as, the averaged link speed plots visualized a massive congestion after the great east Japan earthquake. In addition, hourly right turn ratio per node was high and link speed was low under the torrential downpour, compare to the respective normal condition. Meanwhile, a severe speed reduction was visualized as the time passes on after the earthquake and the right turn ratio per node also has reduced indicating the difficulty of making right turns.

The estimated values of travel time parameter under the both events, indicated the traveller's intention to assess the difference of travel time in links, under congestions. The changing rate clearly showed the severity of the situation after the earthquake. Further, the estimations of the right turn dummy variable showed an increasing difficulty, in turning right under the both scenarios. Finally, the estimated values for sequential time discount rate indicated the transition of traveller's decision making process from the global decisions to myopic decisions.

ACKNOWLEDGMENT: The data used in the aforementioned analysis was provided by the *Vehicle Information and Communication Service Center (VICS)*. So, we thank them. In addition, we would also highly appreciate the kind help of Dr. S. Fukuyama and Dr. Y. Oyama at the University of Tokyo, throughout the process.

REFERENCES

1) Iida, Y., Kurauchi, F. and Shimada, H. : Traffic management system against major earthquakes, *IATSS Research*., Vol. 24, No. 2, pp. 6-17, 2000.
2) Oyama, Y., Chikamatsu, K., Shoji, Y., Hato, E., and Koga, M. : Trajectory-oriented traffic management using sequential discount rate: a case study of the great east Japan earthquake, 11*th* *ITS European Congress*, 2016.
3) IPCC. : Climate Change 2014: Sysnthesis Report, *Contribution of Working Groups I, II and III to the Fifth Assesment Report of the Intergovernmental Panel on Climate Change*, [Core Writing Team, R.K. Pachauri and L.A. Meyer (eds.)], Geneva, Switzerland, pp. 151, 2014.
4) Chengxi, L., Yusak, O. S. and Karlstrom, A. : Weather variability and travel behaviour – what we know and what we do not know, *Transport Reveiws*, 2017.
5) Cascetta, E., Nuzzolo, A. R. F. and Vitetta, A. : A modified logit route choice model overcoming path overlapping problems; specification and some calibration results for interurban networks. *Proceedings of the 13th International Symposium on Transportation and Traffic Theory*, Lyon, France, pp. 697-711, 1996.
6) Ben-Akiva, M. and Bierlaire, M.: Discrete choice methods and their applications to short term travel decisions. In: *Handbook of Transportation Science*, Springer US, pp. 5-33, 1999.
7) Bustillos, B. I., Chiu, Y. C. and Papayannoulis, V. : Pre-Trip and En-Route Multi-Modal Travel Decisions Considering Habitual Travel Times under Unexpected Incident Scenarios, *14th International IEEE conference on Intelligent Transportation Systems*, Wachington, DC, USA, 2011.
8) Chen, H. and Hsueh, C.: A model and an algorithm for the dynamic user-optimal route choice problem, *Transportation Research Part B*, Vol. 32(3), pp. 219-234, 1998.
9) Liu, H. X., Ban, X., Ran, B. and Mirchandani, P. : An analytical dynamic traffic assignment model with probabilistic travel times and travelers' perceptions, *California Partners for Advanced Transportation Technology*, Working papers, 2002.
10) Bliemer, M. C. J. and Taale, H. : Route generation and dynamic traffic assignment for large networks, *First international sysmposium on dynamic traffic assignment*, Leeds, 2006
11) Ng, M. : A dynamic route choice model considering uncertain capacities, Computer-aided civil and insfrastructure engineering, Vol. 27, pp. 231-243, 2012.
12) Gentile, G. and Papola, A. : An alternative approach to route choice simulation: The sequential midels, *European Transport Conference*, 2006.
13) Baillon, J. and Cominetti, R. : Markovian traffic equilibrium. *Mathematical Programming*, Vol. 111, pp. 33-56, 2008.
14) Fosgerau, M., Frejinger, E., and Karlstrom, A. : A link based network route choice model with unrestricted choice set, *Transportation Research Part B*, Vol. 56, pp. 70-80, 2013.
15) Rust, J. : Optimal replacement of GMC bus engines: An empirical model of Harold Zurcher, *Econometrica: The Economic Society*, Vol. 55(5), pp. 999-1033, 1987.
16) Bellman, R. E. : Dynamic programming, *Princeton University Press*, 1957.
17) GeosenseInc. : Geocode Viewer. [Online], Available at: http://www.geosense.co.jp/map/tool/geoconverter.php, 2006.
18) Dijkstra, E. W. : A note on two problems in connexion with graphs. *Numerische Mathematik* , Vol. 1, pp. 269-271, 1959.
19) Dias, C., Miska, M., Kuwahara, M. and Warita, H.: Relationship between congestion and traffic accidents on expressways: An investigation with Bayesian belief networks, *40th Annual Meeting of Infrastructure Planning (JSCE)*, Japan, 2009.

(Received July 31, 2017)